Chiang Mai J. Sci. 2016; 43(2) : 282-287
http://epg.science.cmu.ac.th/ejournal/
Contributed Paper

Characterization of $CdS_{0.9}Se_{0.1}$ Powder by Scanning Transmission Electron Microscopy

Masahiro Kawasaki[a], Thanapat Autthawong[b], Thapanee Sarakonsri* [b,c] and Makoto Shiojiri[d,e]+

[a] JEOL USA Inc., 11 Dearborn Road, Peabody, MA 01960, USA.

[b] Department of Chemistry, Chiang Mai University, Chiang Mai 50200, Thailand.

[c] Materials Science Research Center, Faculty of Science, Chiang Mai University, Chiang Mai 50200, Thailand.

[d] Kyoto Institute of Technology, Kyoto 606-8585, Japan.

[e] Faculty of Engineering, University of Toyama, Toyama 930-8555, Japan.

+ Present address: 1-297 Wakiyama, Kyoto 618-0091, Japan. shiojiri@pc4.sonet.ne.jp

*Author for correspondence; e-mail: tsarakonsri@gmail.com

Received: 15 September 2015
Accepted: 16 December 2015

ABSTRACT

n-type $CdS_{0.9}Se_{0.1}$ powder was produced by mixing and annealing of CdS and Se powders that were prepared by a reflux method using $Cd(CH_3CO)_2{\cdot}2H_2O$, thiourea and ethylene glycol, and by a solution method using SeO_2, ethylene glycol and $NaBH_4$, respectively. The product was supposed to be crystalline $CdS_{0.9}Se_{0.1}$ powder from simulation of X-ray diffraction pattern using CaRine 3.1 program and JCPDS card of CdS (space group $P6_3mc$). Analytical electron microscopy revealed that Cd, S and Se atoms were homogeneously distributed in the powder, which was composed of particles as fine as a few ten nm and in a single crystalline phase, supporting the formation of $CdS_{0.9}Se_{0.1}$. This $CdS_{0.9}Se_{0.1}$ powder is expected to be used as *n*-type thermoelectric materials.

Keywords: electron microscopy, chalcogenides, semiconductor

1. INTRODUCTION

In 1954, Goldsmid and Douglas proposed the use of semiconductor in thermoelectric refrigeration and disclosed good thermoelectric properties of Bi_2Te_3 [1]. Bi_2Te_3-based thermoelectric materials have the highest ZT~1.14 at room temperature and are widely used in heating or cooling devices. ZT is the dimensionless figure of merit to quantify the efficiency of thermoelectric materials and devices, and defined as $ZT = (S^2\sigma/\kappa)T$, where S, σ, κ, and T are the Seebeck coefficient, electrical conductivity, thermal conductivity, and absolute temperature, respectively [2]. Bi_2Te_3/Sb_2Te_3 superlattices produced by the low-temperature deposition achieved ZT as high as ~2.4 at 300 K [3].

A high ZT of ~1.3 at 923 K was reported for 2.5 at.% Na-doped *p*-type PbS with endotaxially nanostructured 3.0 at.% CdS [4]. The effect of CdS and ZnS as second

phases on the thermoelectric properties of the *p*-type PbS was examined. The *ZT* increased with CdS fraction from 0.9 for $Pb_{0.975}Na_{0.025}S$ through 1.1 for $Pb_{0.975}Na_{0.025}S$ + 1.0% and 1.2 for $Pb_{0.975}Na_{0.025}S$ + 2.0%. Materials or devices with higher *ZT* values of 3 or above at room temperature are still needed to make practical thermoelectric cooling or power generation system. CdS has been used as photo catalytic and photo electrochemical materials for solar cell. A considerable improvement in performance has been noted by alloying with Selenium. That is, CdS_xSe_{1-x} is a highly photosensitive and photo luminescent semiconductor applicable to devices such as photo resistors, optical filters, light displays, infrared imaging devices, etc., and its photoelectric properties have been extensively investigated [5-14].

To have a high value of *ZT* for thermoelectric materials, *S* and σ need to be large while κ needs to be small. Se atom has more electrons than S atom. As a result of addition of Se atoms, *S* and σ of the CdS would be increased. In addition, Se atoms with larger atomic radius than S atom would hinder the lattice vibration in the CdS, and then allow to decrease κ. $CdS_{0.9}Se_{0.1}$ is lower in the price of raw materials and the cost for synthesizing than Bi_2Te_3. Therefore, $CdS_{0.9}Se_{0.1}$ could be a new promising material for thermoelectric application. There are no report on the value of figure of merit, *ZT*, as far as we know. We synthesized $CdS_{0.9}Se_{0.1}$ powder to measure physical properties including electric, photoelectric, and thermal conductivities for calculating *ZT*. In this paper, we characterize the structure of a prepared $CdS_{0.9}Se_{0.1}$ powder by means of analytical electron microscopy as well as X-ray diffraction (XRD) method.

MATERIALS AND METHODS

CdS and Se powders as raw materials were produced as follows. The CdS powder was prepared using a reflux method where $Cd(CH_3COO)_2{\cdot}2H_2O$ of 1 mol and thiourea of 1 mol were dissolved in ethylene glycol of 50 ml, separately, and the both of solutions were mixed together so as to be a homogenous solution. The mixed solution was refluxed at a reaction temperature of 250 °C for 8 h. The Se powder was prepared by a solution method where SeO_2 of 1 mol was dissolved in ethylene glycol of 50 ml and then $NaBH_4$ was added gradually in the solution during a reaction time of 8 h in order to reduce SeO_2. For preparation of 1 g of $CdS_{0.9}Se_{0.1}$, the CdS powder of 0.9686 g and the Se powder of 0.0529 g were mixed and ground in a mortar, and then annealed at 700 °C for 10 h under N_2 atmosphere. During the annealing, some Se atoms might be substituted for S atoms, which were released out in a gas phase. The prepared sample was dark red colored in a form of powder. The powder was initially examined by XRD method. Then, it was dispersed with isopropanol onto holey carbon Cu meshes and observed using a JEM-2200FS (with an objective lens of *C*s = 2.0 mm) configured with an incorporated Omega filter, an Oxford 30 mm^2 SiLi EDS detector, and a Gatan US 1000 CCD camera. The energy dispersive X-ray spectroscopy (EDS) analysis was performed using a 1 nm electron beam probe, and high-angle annual dark-field (HAADF) scanning transmission electron microscopy (STEM) was performed using a 0.5 nm probe.

RESULTS AND DISCUSSION

Figure 1 shows XRD pattern of the prepared powder. Since there are no JCPDS cards of $CdS_{0.9}Se_{0.1}$, the XRD pattern of the $CdS_{0.9}Se_{0.1}$ crystal was simulated by CaRine 3.1 program (CaRine Crystallography) for the hexagonal CdS structure where S atoms are

subsituted by Se atoms according to atomic ratio, using JCPDS card No. 41-1049 of CdS (space group $P6_3mc$). The estimated lattice parmaters of the $CdS_{0.9}Se_{0.1}$ crystal was $a = b = 0.4154$ nm and $c = 0.6764$ nm for those of the CdS crystal of $a = b = 0.4141$ nm and $c = 0.6720$ nm in the original card. The simulated X-ray diffraction data for the crystalline $CdS_{0.9}Se_{0.1}$ powder is illustrated in Table 1. This account for the observed diffraction pattern, as shown in Figure 1.

Table 1. X-ray diffraction data simulated for $CdS_{0.9}Se_{0.1}$ using CaRine 3.1 program from JCPDS card No. 41-1049 of CdS (space group $P6_3mc$).

$CdS_{0.9}Se_{0.1}$	2θ	Intensity	*d*	*hkl*
Crystal system : hexagonal	24.73	65.2	3.598	100
Space group : P63mc	26.33	45.8	3.382	002
Space group number : 186	28.07	100.0	3.176	101
Lattice parameters:	36.43	27.7	2.464	102
$a = 0.4154$ nm	43.54	50.4	2.077	2-10
$b = 0.4154$ nm	47.55	50.6	1.910	103
c = 0.6764 nm	50.71	7.6	1.799	200
$\alpha = 90.0000°$	51.60	36.3	1.770	2-12
$\beta = 90.0000°$	52.60	15.2	1.738	201
$\gamma = 120.0000°$	54.20	2.2	1.691	004
Diffraction angle 2θ is	58.03	6.0	1.588	202
for CuK_α	60.44	2.2	1.530	104

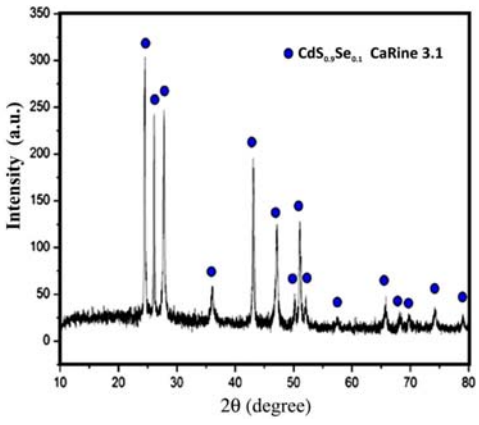

Figure 1. X-ray diffraction pattern of the prepared $CdS_{0.9}Se_{0.1}$ powder. The blue circles indicate the positions of the reflection peaks simulated for crystalline $CdS_{0.9}Se_{0.1}$ powder using CaRine 3.1 program from JCPDS card No. 41-1049 of CdS (space group $P6_3mc$).

EDS mapping analysis was performed for the $CdS_{0.9}Se_{0.1}$ powder shown in Figure 2(a), which is a low magnification zero-loss (0±5 eV) transmission electron microscopy (TEM) image. This image reveals the size and shape of the particles. Figure 2(b) shows the corresponding HAADF STEM image. HAADF STEM images are mainly formed by thermal diffuse scattering of electrons or incoherent imaging of elastically scattered electrons and provides the atomic number (*Z*) contrast, approximately proportional to the square of Z [15, 16]. The contrast is also proportional to thickness of the specimen if it is composed of the same elements. Figure 2(c), 2(d), and 2(e) show the EDS maps of Cd-K, S-K, and

Se-L, respectively. These maps exactly resemble one another, indicating that Cd, S, and Se atoms were homogeneously distributed in the powder, in other words they made a single phase that is $CdS_{0.9}Se_{0.1}$. In these case the HAADF image illustrates the thickness mapping.

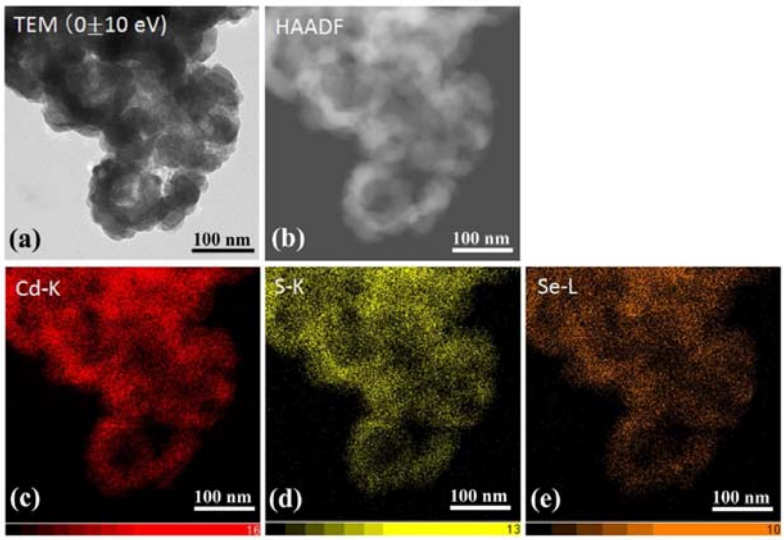

Figure 2. Survey of the $CdS_{0.9}Se_{0.1}$ powder. (a) Zero-loss (0±5 eV) TEM image. (b) HAADF-STEM image. (c-f) EDS maps of Cd-K, S-K, and Se-L.

Figure 3(a) and 3(b) show an energy filtered (EF) TEM image of zero-loss (0±5 eV) and the corresponding conventional TEM image of an area shown in Figure 2, respectively. Figure 3(c) is the EFTEM thickness map, whose intensity is proportional to the local specimen thickness t, that is t/λ. The thickness $t = \lambda \ln (I_T/I_0)$, where I_0 and I_T are the zero-loss and total inelastic electron intensity, respectively and λ is a mean free path of inelastic scattering of electrons [17]. I_0 and I_T were obtained from Figure 3(a) and 3(b). From the histogram shown in Figure 3(d) the average mean thickness was estimated to be $t/\lambda = 0.71 > 0.5$. It means that the specimens is too thick to perform exact EELS measurements without any disturbance of the multiple scattering. In any case, the thickness map indicated in Figure 3(c) exhibits the same contrast with the HAADF image in Figure 2(b). This also confirms a single phase of the present $CdS_{0.9}Se_{0.1}$. The powder comprised particles of a few ten nm in size. These nanoparticles were cohered or connected with each other and made a doughnut-like shape with an outer diameter of 100~200 nm and an inner diameter of 20~50 nm. The doughnuts might form on the holey carbon film as a result of Bénard convection occurring at evaporation of isopropanol during the STEM specimen preparation [18].

A high-resolution (HR) TEM image in a square indicated in Figure 3(a) is shown in Figure 4. Moiré fringes observed in thicker areas indicate that the particles were crystalline. In thin areas of Squares 1 and 2 indicated in Figure 4(a), the $(10\bar{1}0)$ and $(01\bar{1}0)$ lattice fringes and the $(10\bar{1}1)$ lattice fringes of $CdS_{0.9}Se_{0.1}$ crystals were observed. The present $CdS_{0.9}Se_{0.1}$ was a *n*-type conductor. It is very difficult to make *p*-type CdS like

ZnS and ZnO [19], because of strong self-compensation effect ascribed to S vacancies and deep acceptor level in CdS. Rather, the doping of Se which has more electrons and larger atomic radius makes to *n*-type, although *p*-type CdS formed due to doping of Cu [20].

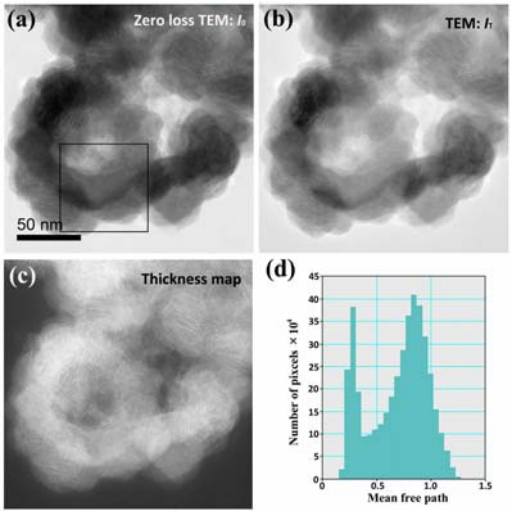

Figure 3. Thickness mapping of the same area with Figure 2. (a) EF-TEM image of zero-loss (0±5 eV). (b) Conventional TEM image. (c) EFTEM thickness map. (d) Histogram of thickness map.

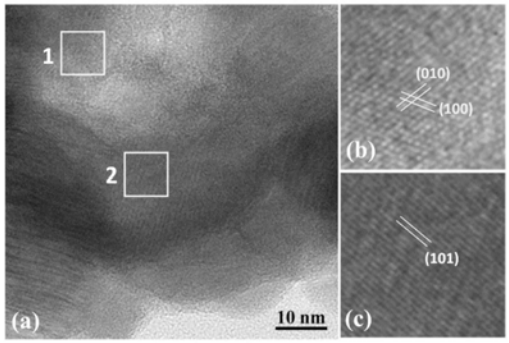

Figure 4. HR-TEM image (0±5 eV) of the area in a square indicated in Figure 3(a). (b) 4-times enlarged image in Square 1. (c) 4-times enlarged image in Square 2.

CONCLUSIONS

We have investigated the structure of $CdS_{0.9}Se_{0.1}$ powder which was prepared by mixing and annealing of CdS and Se powders. The CdS powder was produced by a reflux method using $Cd(CH_3COO)_2{\cdot}2H_2O$ and thiourea (CH_4N_2S) as precursors and ethylene glycol as a solvent, and the Se powder was produced by a solution method using SeO_2 and ethylene glycol and $NaBH_4$ as a reducing agent. We supposed the prepared powder to be $CdS_{0.9}Se_{0.1}$, because its XRD pattern was accounted for by the XRD pattern simulated for $CdS_{0.9}Se_{0.1}$ crystalline powder using CaRine 3.1 program and JCPDS card No. 41-1049 of CdS (space group $P6_3mc$). EDS mapping and TEM/STEM observations for the powder indicated that Cd, S and Se atoms were homogeneously distributed in the powder, and that the powder was composed of particles in a single crystalline phase with Cd, S, and Se, supporting the formation of *n*-type $CdS_{0.9}Se_{0.1}$. The size of the particles was a few ten nm. This n-type $CdS_{0.9}Se_{0.1}$ powder would be applicable to thermoelectric materials.

ACKNOWLEDGEMENTS

We express our deep thanks to Dr. Julie (Hui) Qian, National Institute for Nanotechnology, Canada, for using JEM-2200FS and helping specimen preparation for electron microscopy. Our special thanks are to Prof. Torranin Chairuangsri, Chiang Mai University, for his support and encouragements. This study was partially supported by the National Research University Project under Thailand's Office of the Higher Education Commission (NRU).

REFERENCES

[1] Goldsmid H. and Douglas R., *Br. J. Appl. Phys*., 1954; **5**: 386.

[2] Snyder G.J. and Toberer E.S., *Nature Mater*., 2008; **7**: 105-14.

[3] Venkatasubramanian R., Siivola E., Colpitts T. and O'quinn B., *Nature*., 2001; **413**: 597-602.

[4] Zhao L.D., He J., Hao S., Wu C.I., Hogan T.P., Wolverton C. and et al., *J. Am. Chem. Soc*., 2012; **134**: 16327-36.

[5] Bube R.H., *Phys. Rev*., 1955; **99**: 1105.

[6] Ueno Y., Minoura H., Nishikawa T. and Tsuiki M., *J. Electrochem. Soc*., 1983; **130**: 43-7.

[7] Yukami N., Ikeda M., Harada Y., Nishitani M. and Nishikura T., *IEEE. Tran. Electron Devices*., 1986; **33**: 520-5.

[8] Shevel S., Fischer R., G□ bel E., Noll G., Thomas P. and Klingshirn C., *J. Lumin*., 1987; **37**: 45-50.

[9] Gupta P., Chaudhuri S. and Pal A., *J. Phys. D*., 1993; **26**: 1709.

[10] Rincon M., Sanchez M. and RuizGarcia J., *J. Electrochem. Soc*., 1998; **145**: 35-44.

[11] Grigorieva N., Grigoriev R., Denisov E., Fedorov D., Kazennov B. and Novikov B., *J. Cryst. Growth*., 2000; **214**: 457-9.

[12] Pagliara S., Sangaletti L., Depero L., Capozzi V. and Perna G., *Appl. Surf. Sci*., 2002; **186**: 527-32.

[13] Bhushan S. and Oudhia A., *Ho. Opto-Electron Rev*., 2009; **17**: 30-9.

[14] Oudhia A., Bose P., Vishwakarma V. and Shukla N., *Chalcogenide. Lett*., 2010; **7**: 491-6.

[15] Rickerby D.G., Valdre G. and Valdre U., Impact of electron and scanning probe microscopy on materials research: Springer Science & Business Media; 1999.

[16] Shiojiri M. and Saijo H., *J. Microscopy*., 2006; **223**: 172-8.

[17] Malis T., Cheng S. and Egerton R., *J. Electron Micr. Tech*., 1988; **8**: 193-200.

[18] Kitano M. and Shiojiri M., *Powder. Technol*., 1997; **93**: 267-73.

[19] Chen M.J., Yang J.R. and Shiojiri M., *Semicond. Sci. Technol*., 2012; **27**: 074005.

[20] Kashiwaba Y., Kanno I. and Ikeda T., *Jpn. J. Appl. Phys*., 1992; **31**: 1170.